Journal of Hazardous Materials 183 (2010) 410–420

Contents lists available at ScienceDirect

Journal of Hazardous Materials

journal homepage: www.elsevier.com/locate/jhazmat

Cd(II) adsorption on various adsorbents obtained from charred biomaterials

Zhenze Li[a,*], Takeshi Katsumi[a], Shigeyoshi Imaizumi[b], Xiaowu Tang[c], Toru Inui[a]

[a] GSGES, Kyoto University, Sakyo, Kyoto 606-8501, Japan
[b] Dep. Adv. Interdiscip. Sci., Utsunomiya University, Yoto, Utsunomiya 321-8585, Japan
[c] MOE Key Laboratory of Soft Soils and Geoenvironmental Engineering, Zhejiang University, Hangzhou 310058, China

ARTICLE INFO

Article history:
Received 27 May 2010
Received in revised form 8 July 2010
Accepted 9 July 2010
Available online 15 July 2010

Keywords:
Cadmium
Adsorption
Charred biomaterials
Kinetics
Equilibrium
Modeling

ABSTRACT

Cadmium could cause severe toxicant impact to living beings and is especially mobile in the environment. Biomass is abundant and effective to adsorb heavy metals, but is easy to be decomposed biologically which affects the reliability of long-run application. Several biomasses were charred with and without additives at temperatures less than 200 °C in this study. The prepared adsorbents were further testified to remove Cd(II) from aqueous solution. Equilibrium and kinetic studies were performed in batch conditions. The effect of several experimental parameters on the cadmium adsorption kinetics namely: contact time, initial cadmium concentration, sorbent dose, initial pH of solution and ionic strength was evaluated. Kinetic study confirmed (1) the rapid adsorption of Cd(II) on GC within 10 min and (2) the following gradual intraparticle diffusion inwards the sorbent at neutral pH and outwards at strong acidic solution. The grass char (GC) was selected for further test according to its high adsorption capacity (115.8 mg g^{-1}) and affinity (Langmuir type isotherm). The Cd(II) removal efficiency was increased with increasing solution pH while the highest achieved at sorbent dosage 10.0 g L^{-1}. The ionic strength affects the sorption of Cd(II) on GC to a limited extent whereas calcium resulted in larger competition to the sorption sites than potassium. Spectroscopic investigation revealed the adsorption mechanisms between Cd(II) and surface functional groups involving amine, carboxyl and iron oxide. The long-term stability of the pyrolyzed grass char and the potential application in engineering practices were discussed.

1. Introduction

Heavy metal pollution is a common environmental problem facing many places worldwide with the rapid development of economies and industries [1]. Although various routines were observed responsible for the transport of heavy metals in the environment, anthropogenic wastewater containing heavy metals remains to be the main source of water pollution in the developing countries [2].

Cadmium is not a necessary nutritional element for and could cause severe toxicant effect to living beings at very low doses compared to other heavy metals [2,3]. Therefore, the maximum allowable concentration of Cd(II) in drinking water is strictly legislated in many countries. Cd(II) is especially mobile in both the ground and the estuary, and could be enriched in the seeds of plants (e.g. rice) and in the aquatic livings (e.g. fish and algae) [1,4]. Christensen investigated the leaching of several heavy metals from soil columns and found that most of the metals were retained in the upper few centimeters except cadmium which was present in the effluent [5]. Because it always takes many expenses to get the polluted ground remediated naturally or intentionally, the best way to prevention is to remove the pollutant from the point source [6,7].

Various materials have been reported to remove heavy metals from wastewaters. Natural soils [6,7], minerals [2,8], tailing wastes and biomasses [9–12] were widely investigated using both the original form and the modified forms. As a kind of chemically active and unstable material, biomass always appears to have strong adsorption affinity and high adsorption capacity towards heavy metals. On the other hand, one major concern about biomasses was their tendency to be decomposed biologically, which limits the applicability of such materials in the long-run view point.

Zoysia is a genus of eight species of creeping grasses native to southeastern and eastern Asia (north of China and Japan) and Australasia. Because of its tolerance to wide variations in temperature, sunlight, and water, zoysia grasses are widely used for lawns in temperate climates worldwide, i.e. eastern Asia, North America, Africa, etc. [13]. In Japan, the household garbages are well divided, packed and collected before proper disposal. The large quantity of lawn grass makes it possible to utilize and resourcify these biomass wastes in a more economic pattern.

Biodiesel has caused increasing attention from both academia and industries. Pyrolysis of natural hydrocarbons such as wood

* Corresponding author at: GSGES, Kyoto University, Yoshida Campus, Sakyo, Kyoto 606-8501, Japan. Tel.: +81 75 753 5116; fax: +81 75 753 5116.
E-mail address: lazyhero@live.cn (Z. Li).

0304-3894/$ – see front matter © 2010 Elsevier B.V. All rights reserved.
doi:10.1016/j.jhazmat.2010.07.040

and grass has been tried to serve this purpose [14–17]. Most of these efforts are involved with the volatile/semi-volatile parts of the liquid fuels [14], little is about the utilization of residual chars. The authors have proposed a method to prepare adsorbents with improved stabilities as well as enhanced adsorption performances. The method has been applied to activate leaf, wood and soil, all exhibiting novel attractive features [18,19]. This paper attempts to broaden the scope of the application of the treatment method to grass, another leaf and wood species.

Several biomasses, i.e. pine wood, pine needle and *Zoysia japonica* grass, were partially pyrolyzed adsorbents in anoxic conditions at 150–200 °C. These materials were tested by Batch method regarding their adsorption behaviors towards Cd(II). The effect of several experimental parameters on Cd(II) adsorption namely contact time, initial Cd(II) concentration, sorbent dosage, initial solution pH and ionic strength was systematically investigated. The optimum condition for Cd(II) adsorption was determined finally. SEM, SEM-EDX and FT-IR were used to characterize the adsorbents and to investigate the adsorption mechanism of Cd(II) on the charred biomaterials. The adsorbent with the best Cd(II) adsorption performance was determined and further compared with the reported materials.

2. Materials and methods

2.1. Preparation of adsorbents

The grass (*Z. japonica*) was sampled from a mowed lawn in Utsunomiya University in October, 2009. The grass was left under sunshine to air dry and then collected, cut with scissor to pieces <0.5 cm in length, and heated from room temperature to 200 °C with a temperature increment of 20 °C min^{-1} and then remained for 0.50 h in semi-anoxic condition. No preservative gas atmosphere was supplied during the pyrolysis process in order to simplify the preparation process. The volatile components that would be produced under increased temperatures were allowed to release from the reactor (50 cm × 15 cm × 15 cm) via an opened hole at 0.5 cm in diameter. The hole was on the top of the reactor and was covered by aluminum foil to allow the release of gas from inside to outside while preventing the reverse movement of the air.

Pine wood chip (length × width × thickness < 0.5 cm × 0.2 cm × 0.005 cm) was purchased from a local wood factory (Utsunomiya city, Japan). The initial water content of the wood chip was determined at around 8%. The wood was heated at 200 °C to prepare wood char (WC) following the same preparation processes to GC. As a comparison, ferric laden wood char (FLWC) was prepared by pyrolyzing wood chip with iron nitrate (mass ratio of iron/wood at 10%, analytical grade, Kyokaxia Company, Japan). Iron oxide was coated on the surface of FLWC with ground crystal of $Fe(NO_3)_3{\cdot}9H_2O$ rather than with concentrated solution, since the melting point of iron nitrate nonahydrate at 47.2 °C allows the iron salt to diffuse within the prepared chars. Another series of ferric laden wood char (FLWC1) was also prepared following the abovementioned procedures, except for the treatment temperature (at 150 °C) and the pyrolysis duration (2.0 h), which were aimed to investigate the effect of treatment temperature on the adsorbent properties. The chars were cooled to room temperature naturally, pulverized with a mortar, screened to pass 200 μm mesh and then collected in Ziploc sealed plastic bags for storage.

Pine needle was collected from those fallen on the ground in the campus of Utsunomiya University in October, 2009. The pine needle was air dried, cut into short pieces <0.5 cm in length, and then heated with grounded powder of $Fe(NO_3)_3{\cdot}9H_2O$ (mass ratio of iron/pine needle at 10%, analytical grade, Kyokaxia Company, Japan) to prepare the ferric laden pine needle char (FLPNC). The preparation conditions were identical to the previous ones.

The treatment temperature for sample preparation in this study was carefully determined according to the literatures. The pyrolysis-field ionization study showed that the stem of grass would lose its weight rapidly at temperatures between 150 and 250 °C. Further increase in temperature resulted in another two peaks of mass loss at 290 and 350 °C, with the ash residual formed at $T > 500$ °C [20]. In order to preserve valuable functional groups as well as to get rid of decomposable organic components, a treatment temperature at 200 °C was chosen in this study to partially pyrolyze the grass. Our previous experiences in activation of leaf and pine wood confirmed the positive effect of this temperature [21].

The additive to wood char was also selected after careful thought. Salt was reported to proceed the liquefaction of wood at comparatively low temperatures [22]. Richards and Zheng reported that transition metals could act as catalyzer during the low-temperature pyrolysis of cellulose [23]. The transition metal cation could be partly reduced to lower oxidation state which is known to catalyze the gasification of chars. Hence, it is anticipated that ions such as iron and copper (or their reduction products) will catalyze the gasification of chars in the subsequent high temperature gasification [23].

2.2. Characterization of adsorbents

The microstructures of the prepared adsorbents were investigated by Scanning Electron Microscopy (SEM) using Hitachi SEM-S 4500 (Japan, Hitachi Ltd.). The elemental constituents on the surface of the adsorbents were analyzed by EDX facility which is attached to the SEM. All these samples were coated with Pr–Pt under vacuum conditions (6 Pa, 15 mA) for 90 s before being subjected to SEM observation.

The functional groups of each sample were analyzed using FT-IR spectroscopy (FT/IR-4100 type A, Japan Spectroscopy). The samples were firstly dried at room temperature under vacuum condition (<10 Pa) for at least 10 min. One part of sample was mixed with five parts of KBr, ground to fine powder, and was compressed into translucent lens in a mold under pressure of 20 kPa for 30 s. The lens was transferred to FT-IR facility to determine the transmittance percentage.

2.3. Adsorption kinetics study

2.3.1. Effect of contact time and initial cadmium concentration

Three 20.0 mL aliquots of Cd(II) solution with initial concentrations at 2.5, 5.0 and 10.0 mg L^{-1} were separately mixed with 0.020 g GC powder in conical flasks that were previously cleaned. The mixture was equilibrated in an agitator at 25.0 °C. The equilibration duration of the mixture was 10, 30, 60, 120 and 180 min, respectively for relevant samples. The mixture was then separated using a membrane filter (0.45 μm). The concentration of Cd(II) in the supernatant was determined by ICP-MS. Two sets of test were conducted to compare the effect of pH: one was fixed at 2.7 and the other at 6.8. Each sample was duplicated with blank.

2.3.2. Effect of sorbent dosage

Increased amounts of prepared chars were measured from 0.010, 0.020, 0.040, 0.100 to 0.200 g, separately, and then individually transferred to different flasks. Aliquots of 20.0 mL Cd(II) solution (5.0 mg L^{-1}) were filled to the flasks with the adsorbents. The flasks were capped and placed in a shaking bed for continuous equilibration for 24.0 h. Afterwards, the agitator was stopped and the mixture was separated using a 0.45 μm filtration membrane.

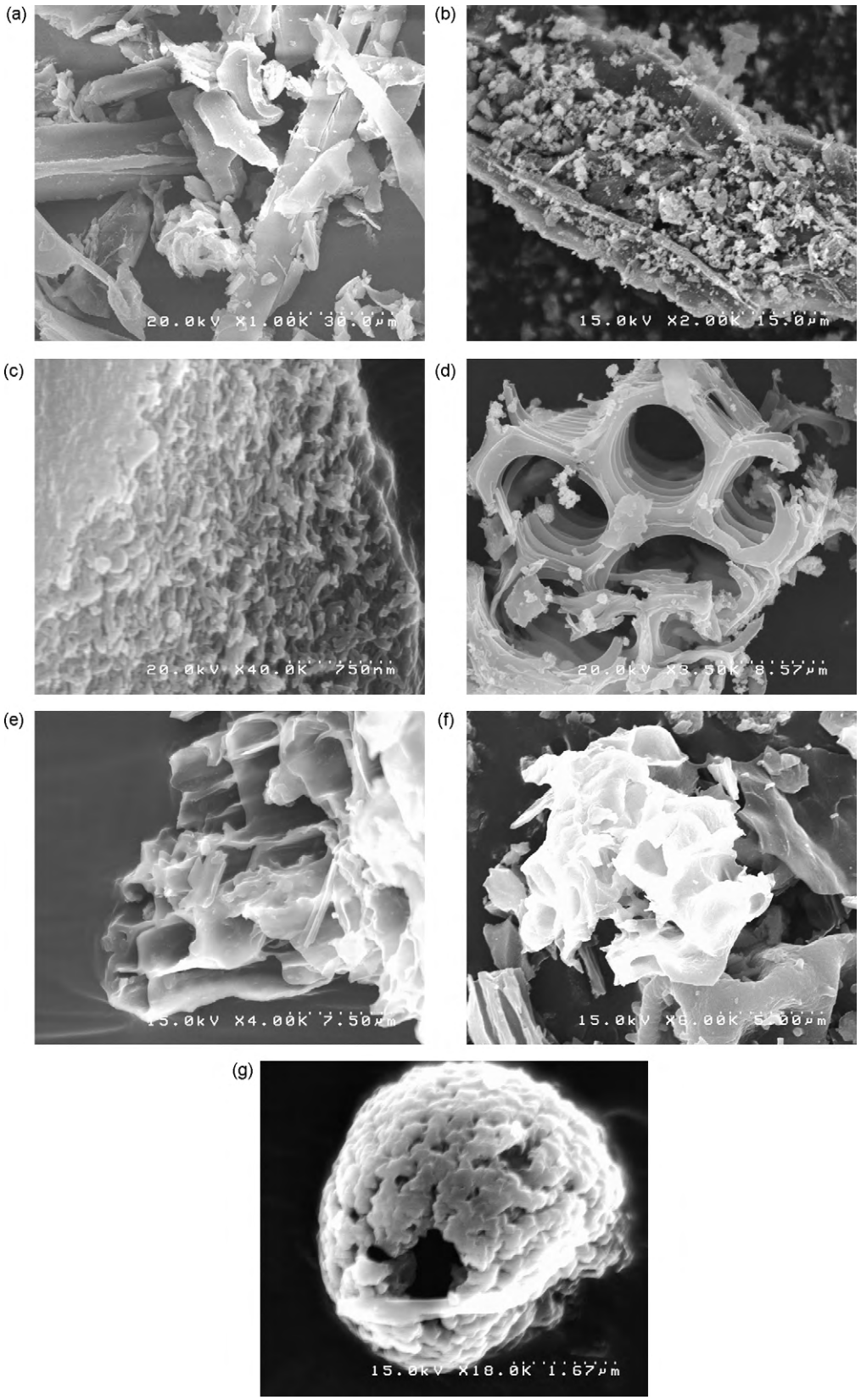

Fig. 1. SEM photos of various chars (a: WC; b: FLWC; c: FLWC1; d: FLPNC; e–g: GC).

The concentration of Cd(II) in the clear solution was determined by Inductively Coupled Plasma Mass Spectrometer ICP-MS (ICP S4500, Shimazu, Japan). Each test was duplicated and the results were averaged.

2.3.3. Effect of solution pH

Solutions containing predetermined amount of Cd(II) (target concentration is 5.0 mg L^{-1}) were prepared and transferred to relevant cubic flasks. The initial volume of the solution was sampled at

Table 1
Preparation conditions and elemental concentrations on the surface of various adsorbents.

Sorbents	Components	Activation temperature (°C)	Yield efficiency (%)	Surface atomic concentration (%)			
				C	N	O	Fe, Al, Si, Ca, etc.
WC	Pine wood	200	55.27	97.46	0.00	2.54	0.00
FLWC	Pine wood, iron nitrate	200	28.78 (char) 20.36 (Fe_2O_3)	89.63	0.00	10.02	0.33 (Fe)
FLWC1	Pine wood, iron nitrate	150	35.49 (char) 26.48 ($Fe(OH)_3$)	74.19	0.00	21.20	4.62 (Fe)
FLPNC	Pine needle, iron nitrate	200	35.11 (char) 20.36 (Fe_2O_3)	96.75	0.00	3.12	0.13
GC	Grass *Z. japonica*	200	31.25	34.47	46.76	17.53	1.24

15.0 mL, equivalent to 3/4 of the total volume required for the Batch test (20.0 mL), to allow the pH adjustment. Concentrated HNO_3 and NaOH solutions (0.0001–0.01 M) were used to regulate the initial pHs from 2.0 to 11.0 with an increment of 1.0. After that, the solution volume was finally adjusted to 20.0 mL with distilled water. An aliquot of 0.020 g GC was added to the prepared Cd(II) solution. The mixture was equilibrated for 24.0 h at 25 °C. Finally the mixture of sorbent and solution was separated by membrane filtration. The supernatant was sampled to determine the equilibrium Cd(II) concentration by ICP-MS and the equilibrium pH by glass electrode pH meter (Horiba, Japan). Each sample was duplicated with blank.

2.3.4. Effect of ionic strength

An aliquot of Cd(II) solution (20.0 mL) at 5.0 mg L^{-1} was mixed with 0.020 g GC. The ionic strength was separately adjusted to 0.001, 0.01, 0.05, 0.1, 0.2, 0.3, 0.4 and 0.5 M using concentrated KCl and $CaCl_2$ solution. The mixture was equilibrated at 25.0 °C for 24.0 h and then separated for ICP test to determine the equilibrium Cd(II) concentration. Each sample was duplicated to average the results.

2.4. Adsorption equilibrium study

Different chars were all weighed at 0.020 g and transferred to flasks with 20.0 mL Cd(II) solutions at increased initial concentrations from 1.25 to 200.0 mg L^{-1}, separately. Two series of Batch tests were conducted with the initial pH separately at 2.7 and 6.8 which were adjusted by 0.0001–0.01 M HNO_3 and NaOH solutions. The flasks were tapped, placed in an agitator and then equilibrated at 25 °C for 24.0 h. The equilibrium concentration of Cd(II) was determined by ICP-MS after being separated with 0.45 μm membrane filters. Each test was duplicated with blank samples.

3. Results and discussion

3.1. Characterization

Fig. 1a–f shows the SEM photos of the prepared biomaterial chars. The grounded WC as shown in Fig. 1a appears to have broken segments in both wedge and spherical shapes. But micropore was not observed in these particles. Fig. 1b shows the coarse surface of FLWC. Fine particles ($d < 1.5$ μm) were found to cover almost the total surface of chars, indicating a successful coating of iron oxide on the surface of wood char. Micropore in irregular forms was present in FLWC and was expected to give rise to the specific surface area and pore volume of this sorbent. Similar to FLWC, the surface of FLWC1 (Fig. 1c) was also coarse with fine iron hydroxide coating. But its surface appeared to be smoother than that of FLWC, indicating a less degree of dehydration occurred at lower treatment temperature. As to FLPNC shown in Fig. 1d, abundant pores were observed with uniform diameters around 7 μm. Iron oxide particles were present outside the micropores, sized around 1.7 μm in diameters. The pore size of FLPNC was much larger than that of GC. Besides, the pores in FLPNC were connected rather than closed as shown by GC. These features might restrict its capacity to absorb toxicant ions from bulk solution. Fig. 1e shows the cross-section of one GC particle possessing abundant mesopores at 3 μm in diameter. Fig. 1f shows a broken particle of GC, owning multi-dimensionally oriented pores. Fig. 1g shows another fine particle of GC, consisting of silicate and aluminate with micropores less than 1 μm in diameter. According to the microscale morphology of the different chars, the GC was anticipated to have better adsorption performance than the others.

Table 1 shows the preparation conditions and yield efficiencies of the prepared adsorbents. It is obvious that the yield efficiency is higher for samples prepared at lower temperatures. The char yield of FLWC was 6.71% less than that of FLWC1 in spite of limited temperature difference (50 °C). This behavior is in agreement with our previous studies [19,21]. The addition of an oxidant, iron nitrate, decreased the yield of wood char, from 55.27% to 28.78% at 200 °C. The yield of GC (31.25%) was less than that of WC (55.27%), consistent with the thermostability of the biomasses. Wood can resist long-term microbial digestion as the constituent like lignin and semi-cellular are all well crystallized and hard to decompose. But grass seems to be easily digested by microbes and herbivores due to its high content of nitrogen and phosphate [24,25].

Table 1 also shows the chemical compositions of the surface of these adsorbents. The mass concentrations of various elements were calculated on the basis of the EDX result. The mass concentration of nitrogen even reaches a surprisingly high value as 46.76% in GC while being absent in all the other chars. The oxygen content also differs from each other among these adsorbents. There are 21.20, 17.53 and 10.02% of oxygen detected in FLWC1, GC and FLWC, separately. But only 3.12 and 2.54% of oxygen are detected in

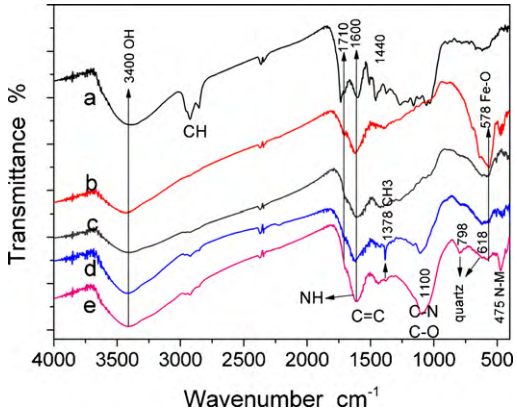

Fig. 2. FT-IR spectra of various adsorbents (a: WC; b: FLWC; c: FLWC1; d: FLPNC; e: GC).

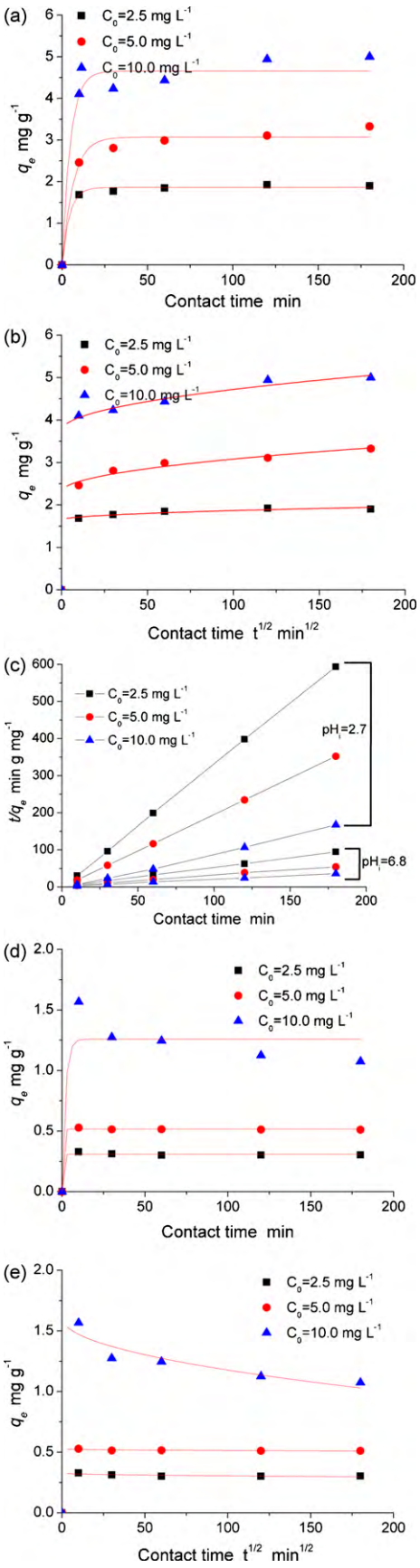

FLPNC and WC. Wood char has less content of oxygen than wood, corresponding to the reported data [22,26]. The increase of oxygen concentration in ferric laden chars is likely to come from the coated iron oxide or iron hydroxide. With the same molar content of Fe, the molar content of O was higher in $Fe(OH)_3$ than in Fe_2O_3, which might explain the higher O % in FLWC1 than in FLWC.

Fig. 2 shows the FT-IR spectra of various adsorbents prepared in this study. The bands at 1600, 1580, 1500 and 1450 cm^{-1} could be assigned to benzene ring which was abundant in WC due to their strong IR absorption. The IR bands related to benzene ring were decreased in FLWC and FLWC1 after treated with iron nitrate. Bands at 2930, 2859 and 1736 cm^{-1} that were found in IR spectrum of WC were attributed to alkyl group –CH, indicating that the pyrolysis temperature was not enough to completely remove these groups from the WC. This observation could explain the high yield efficiency of WC at 200 °C. But the additive iron nitrate could enhance the decomposition degree of wood char since the IR bands of group –CH in these two samples were almost absent in Fig. 2.

Bands at 641, 578 and 470 cm^{-1} could be linked to the coated ferrous oxide, –Fe–O group. The IR pattern of FLWC1 differed from that of FLWC especially at wavenumbers less than 500 cm^{-1}, where the band at 470 was absent in the former solid, confirming the effect of treatment temperature on obtained functional groups of the adsorbents.

In the IR spectra of grass char, a sharp band at 475 cm^{-1} was observed. The writers believe this group should be related to the abundant nitrogen contained in GC, although direct and solid proofs are lacked in the current stage. High intensity bands were found at wavenumbers 1600–1630 and 1100 cm^{-1}, which could be assigned to both C–O bonds and amine groups. Considering the high percent of nitrogen content in GC determined by SEM-EDX, abundant amine groups could be expected to be present in GC. This group has been reported to be effective sorption site for heavy metal adsorptions. A hypothesis could be proposed: chars obtained from heated grass might be applicable in the treatment of heavy metals containing wastewaters.

The wide and strong shoulder at 1710 cm^{-1} could be assigned to C=O group, which was present in WC (strong), GC (strong) and FLWC (weak). Correlated to the broad absorption pattern at 3400 cm^{-1} relevant to OH group, abundant –COOH groups might be available in both WC and GC samples. The band at 1600 cm^{-1} present in all the chars could be assigned to C=C stretching vibration, confirming that these biomasses were pyrolyzed under the preparation conditions in this study.

3.2. Adsorption kinetics

3.2.1. Effect of contact time and initial cadmium concentration

Fig. 3a–e shows the test data of kinetic Cd(II) adsorption on GC at different initial pHs along with the simulated curves. It is obvious that a higher initial Cd(II) concentration gave rise to the adsorption amount, but delayed the time required to equilibrate the adsorption process. Solution pH has significant effect on (1) Cd(II) adsorption amount with nearly 5-fold difference observed in this study; and (2) Cd(II) adsorption behavior with completely different patterns present in the kinetic sequence.

Fig. 3. (a) Kinetic adsorption of Cd(II) on GC and fitted curves with pseudo-first order kinetic model (pH$_i$ = 6.8; dosage 0.10 g L^{-1}; T = 25.0 °C). (b) Kinetic adsorption of Cd(II) on GC and fitted curves with intraparticle diffusion model (pH$_i$ = 6.8; dosage 0.10 g L^{-1}; T = 25.0 °C). (c) Kinetic adsorption of Cd(II) on GC and fitted curves with pseudo-second order kinetics model (pH$_i$ = 2.7 or 6.8; dosage 0.10 g L^{-1}; T = 25.0 °C). (d) Kinetic adsorption of Cd(II) on GC and fitted curves with pseudo-first order kinetic model (pH$_i$ = 2.7; dosage 0.10 g L^{-1}; T = 25.0 °C). (e) Kinetic adsorption of Cd(II) on GC and fitted curves with intraparticle diffusion model (pH$_i$ = 2.7; dosage 0.10 g L^{-1}; T = 25.0 °C).

Table 2
Kinetics model constants for Cd(II) adsorption by GC.

Constants	C_0 (mg L^{-1}) (pH$_i$ 2.7)			C_0 (mg L^{-1}) (pH$_i$ 6.8)		
	2.5	5	10	2.5	5	10
1st order kinetics						
q_e (mg g^{-1})	0.31	0.52	1.26	1.86	3.07	4.66
k_1 (min^{-1})	1.57E4	1.54E2	0.50	0.23	0.16	0.21
R^2	0.990	0.999	0.896	0.995	0.98	0.98
2nd order kinetics						
q_e (mg g^{-1})	0.30	0.51	1.05	1.93	3.38	5.14
k_2 (g mg^{-1} min^{-1})	−5.68	−5.56	−0.16	0.26	0.05	0.03
R^2	1.00	1.00	1.00	1.00	1.00	1.00
Intraparticle diffusion model						
k_{int} (mg g^{-1} min$^{-1/2}$)	−0.002	−0.001	−0.043	0.022	0.077	0.097
C_{int} (mg g^{-1})	0.33	0.53	1.61	1.65	2.31	3.75
R^2	0.65	0.65	0.86	0.87	0.94	0.96

In accordance with the study on pH effect, a lower pH greatly decreased the adsorption amount. At pH$_i$ 2.7, the final Cd(II) adsorption amount on GC after equilibrated for 3.0 h was determined to be 0.309, 0.516 and 1.074 mg g^{-1} for solutions with C_0 at 2.5, 5.0 and 10.0 mg L^{-1}, respectively. At acidic conditions, abundant hydrogen ions could result in strong competition to Cd(II) about the available adsorption sites on the adsorbent. Since GC has plenty of micropores besides surface active functional groups, solute could also be fixed in a manner of pore-filling adsorption.

Normally, the amount of metal adsorbed increases with the increase in the contact time. But the adsorption amount was found to decline gradually at C_0 = 10.0 mg L^{-1} and pH$_i$ = 2.7, which might be attributed to the effect of strong acid by (1) partly dissolving the solid particles and (2) slowly diffusing into the micropores to make the previously fixed Cd(II) released into the solution again.

Although the overall trend of Cd(II) adsorption appeared to be opposite to each other at acidic and neutral pHs regarding the kinetic effect, a rapid adsorption occurred within 10 min of contact between the solute and the adsorbent. For solutions with C_0 < 10.0 mg L^{-1}, the equilibration was obtained within 0.50 h. A higher initial concentration ($C_0 \geq$ 10.0 mg L^{-1}) will increase the equilibration duration to more than 3.0 h.

These data were fitted by three kinetic models: pseudo-first order kinetics, pseudo-second order kinetics and intraparticle diffusion model as shown in Fig. 3a–d. Table 2 shows the calculated model constants and the correlation coefficients.

The pseudo-first order kinetic equation is [27]:

$$C_s^e = C_s(1 - e^{-k_1 t}) \quad (1)$$

where C_s^e and C_s are the amounts of adsorbate per unit weight of adsorbent at equilibrium and any time t, respectively (mg g^{-1}), and k_1 the constant of pseudo-first order rate (min^{-1}).

The pseudo-second order kinetic equation is in the form of [27]:

$$C_s = \frac{1 + k_2 q_e t}{k_2 q_e^2 t} \quad (2)$$

where k_2 (g g^{-1} min^{-1}) is the relevant rate constant and q_e the predicted adsorption capacity (mg g^{-1}).

The intraparticle diffusion model assuming an adsorption in terms of pore-filling pattern is expressed as [27,28]:

$$C_s = k_{int} t^{1/2} + C_{int} \quad (3)$$

where k_{int} is the constant of the relevant adsorption rate (mg g^{-1} min$^{-1/2}$), and C_{int} is the intercept of the kinetic curves (mg g^{-1}).

Pseudo-second order kinetics appeared to fit the test data with usually higher correlation coefficients than the other two models since the correlation coefficient was very close to 1.0. The calculated sorption capacity was close to each other for the first and second order kinetics, whereas those predicted by the latter were a bit less and higher than those by the former model in situations with pH$_i$ at 2.7 and 6.8, respectively. The predicted sorption rate k_2 was negative value and was increased with increasing solute concentration in acidic conditions, but turned to be positive value and decreased with increasing solute concentration in alkaline conditions. The sorption dynamics in these two situations must be significantly different. The negative sorption rate meant that the Cd(II) was released from the sorbent during the observation period.

For the intercept C_{int} in intraparticle diffusion model, McKay et al. have viewed it to be proportional to the extent of the boundary layer thickness of the adsorbent [29]. After reviewing more than 80 literatures, Wu et al. found that most of the reported intercepts were positive and there was always a rapid adsorption at the beginning of adsorption [28]. Our results were in accordance with these viewpoints. The negative adsorption rate k_{int} at pH$_i$ 2.7 further verified the speculation that a rapid adsorption at the initial stage was followed by a gradual dissolution of the solid matrix.

Because we did not detect the sorption dynamics within the very short time after the solute and sorbent contacted, the preliminary sorption stage could only be imagined, but rationally expected, to take place with a very high rate. This is totally possible since the sorption of Cd(II) on GC is mainly engaged with chemisorptions which is a kind of fast reaction. Taking the special porous structure of GC into account, the adsorbed Cd(II) could be partly tapped in the micropores of GC. Therefore, the adsorption of Cd(II) on GC could be considered to be via (1) surface active functional groups like amine and carboxyl and (2) intraparticle diffusion inwards the micropores. The first step dominates at low Cd(II) concentrations while the latter step at high Cd(II) concentrations. These speculations are in agreement with the reported mechanisms [2,19,30].

3.2.2. *Effect of sorbent dosage*

Fig. 4 shows the effect of adsorbent dosage on Cd(II) removal percentage. GC showed the highest Cd(II) adsorption percentage at dosage >5.0 g L^{-1}, reaching 98.0% at dosage 10.0 g L^{-1}. Samples of FLPNC, WC and GC could remove more than 18% of Cd(II) from the solution at dosage 0.5 g L^{-1}. Further increase in dosage resulted in a little increase in *R*%, but all less than 50% at dosage 10 g L^{-1}. The adsorbents FLWC and FLWC1 behaved in a similar manner, the *R*% of the both increased steadily with increasing dosages. Therefore GC was determined to be the most potential and prospective adsorbent within these adsorbents.

Further investigation in the equilibrium pH (pH$_e$) showed that GC could maintain a stable pH$_e$ around pH 6.0 at dosage >5.0 g L^{-1}. This helped to improve its adsorption performance because a moderate pH is critical to fix heavy metals onto the adsorbent. On the other hand, 98% removal of Cd(II) by GC appeared to be

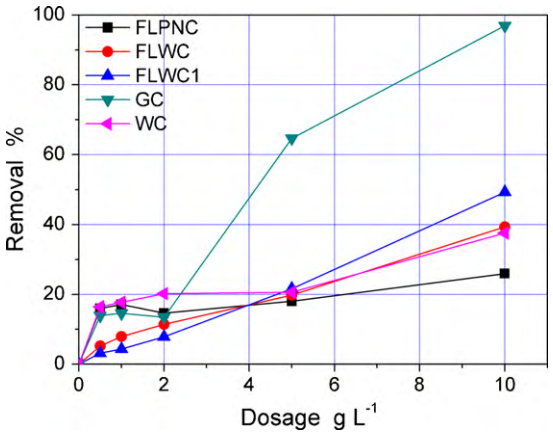

Fig. 4. Effect of adsorbent dosage on Cd(II) adsorption on various adsorbents (C_0 = 5.0 mg L^{-1}; pH_i = 2.7; T = 25 °C; t = 24 h).

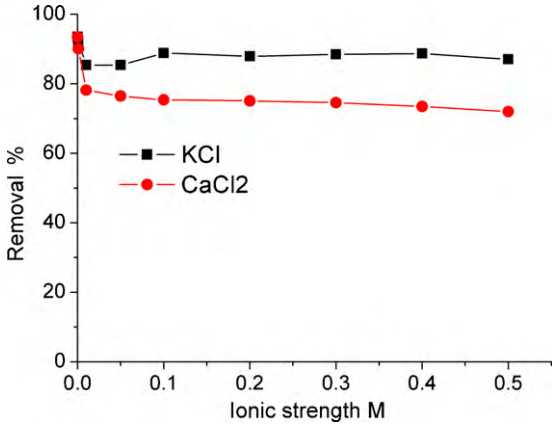

Fig. 6. Effect of ionic strength on Cd(II) removal by GC (C_0 = 5.0 mg L^{-1}; pH_i = 6.8; T = 25.0 °C; t = 24.0 h; dosage 1.0 g L^{-1}).

better than that by quaternary loess reported by Wang et al. [2]. The sorption capacity has been found to be closely related to the surface properties of sorbents as well as solution pHs. As to Cd(II), the alkaline sites on the sorbent are likely to be preferential bonding sites. It is well known that iron oxide has positive zeta potentials at pHs <7–8, therefore the coating of iron oxide would not give rise to the surface alkalinity. Instead, the active surface hydroxyl groups would be reacted with iron. This could explain the observed sorption affinity of Cd(II) on these materials. The pine needle char has a problem in hydrophilicity and thus not all of the pore structures are available to Cd(II) sorption. GC has special structures as confirmed by SEM. The surface function groups like amine and carboxyl help to maintain a high hydrophilicity and high buffering capacity. These properties might both be enhanced at increased dosages. The sharp increase in sorption percentage of Cd(II) on GC could thus be reasonably expected.

3.2.3. Effect of solution pH

Fig. 5 shows the effect of solution pH on Cd(II) adsorption and the relationship between the initial and the equilibrium pH. A rapid increase in the removal percent of Cd(II) from 10 to 90% was observed at 4 < pH < 6 in the presence of GC. Using Visual MINTEQ software, the precipitation behavior of Cd(II) in aqueous solution was modeled and the predicted precipitating edge was around pH 9.25, which was much higher than the equilibrium pH (≈6.50) of GC–water slurry. The sorption of Cd(II) on GC is preferential compared to the precipitation of Cd(II) in the form of $Cd(OH)_2$. The strong affinity and bonding intensity were further verified in Fig. 5.

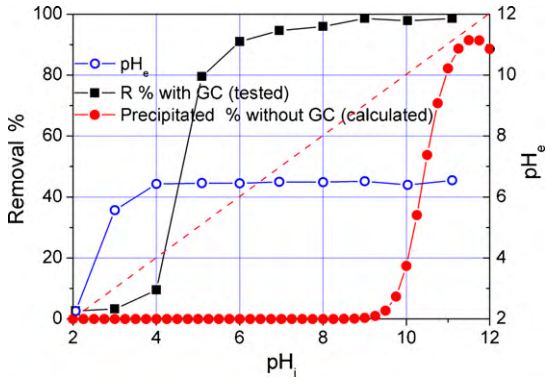

Fig. 5. Effect of initial pH on Cd(II) removal percent and equilibrium pH (C_0 = 5.0 mg L^{-1}; dosage 1.0 g L^{-1}; T = 25.0 °C; t = 24.0 h; solid circle indicates the precipitated percent of Cd(II) in aqueous solution without adsorbent, calculated by Visual MINTEQ software, using 1 mM $Cd(NO_3)_2$, 25 °C, ionic strength at 0.01 M).

The prepared GC appears to be effective to remove Cd(II) in a wide range of pH conditions ranging from 4.0 to 11.0, which might be promising in wastewater treatment. The sorbents laden with Cd(II) could be treated with concentrated acid solution to remove the sorbed metals and further retrieve the sorption capacity.

The pH_e was found to become constant around pH 6.50 rapidly after pH_i increased to and kept higher than 4.0. The points of zero charge (pH_{zpc} values) of GC could be determined by the pH drift method following Yang et al. when the $pH_i = pH_e$. From Fig. 5, the pH_{zpc} could be 6.50 [31]. Although the surface charge of the adsorbent is a physical measure, it could be further related to the surface functional groups in a chemical manner. The coexistence of amine and carboxyl groups helps to maintain a high pH buffering performance. A high buffering capacity of GC towards acid solution can be confirmed. At high pHs > 6.50, the complexation of Cd(II) with OH^- and the deprotonation of –COOH group would exhaust OH^- and thus decrease solution pH, resulting in a lower pH_e. In acid solutions at pH < 6.50, the surface of the GC could be positive due to the protonation of surface functional groups, i.e. from $–NH_2$ to $–NH_3^+$, which might increase the pH_e. The high buffering capacity of GC determines its critical role in metal uptake. Maintaining a equilibrium pH close to neutral condition benefits the sorption of Cd(II) and at the same time avoids the competitive effect of other cations.

3.2.4. Effect of ionic strength

Fig. 6 shows the effect of ionic strength on Cd(II) adsorption on GC. An obvious negative effect could be observed at I < 0.1 M for KCl solution, where the removal percentage of Cd(II) was decreased from 92.16 to 85.40 and 85.43% with increasing ionic strength from 0.001 to 0.01 and 0.05 M, separately. However, further increase in ionic strength from 0.05 to 0.1 and 0.5 M increased the removal percent a bit from 85.43 to 88.89 and 87.05%, separately. As to $CaCl_2$ solution, the effect of ionic strength on Cd(II) sorption was much more obvious than that caused by K solution. The sorption percent of Cd(II) declined steadily from the original 93.5 to 78.21% with increasing Ca concentration from 0.0 to 0.01 M. Further increase in Ca concentration imposed much less competitive effect on Cd(II) adsorption on GC while the R% was reduced from 78.2 to 72.1% by 50 times increase in Ca concentration from 0.01 to 0.5 M.

K^+ could form innersphere complexes with most of the inorganic surfaces because of its small hydrated ionic size [32]. The inhibitory effect of K^+ on Zn sorption has been previously reported for various kinds of soils. In this study, we also observed similar competitive effect from KCl on Cd adsorption on GC. On the other hand, Cd adsorption on GC was enhanced by KCl at higher ionic strengths I > 0.05 M, possibly because of specific adsorption of Cd–Cl complex ions [32]. Naidu et al. observed negative effect of $Ca(NO_3)_2$ on Cd(II)

Table 3
Isothermal model constants for Cd(II) adsorption isotherms by various adsorbents.

Samples	Freundlich		R^2	Langmuir		R^2	Sips			R^2	Observed sorption capacity ($mg\,g^{-1}$)
	K_F ($mg\,g^{-1}$)	n		Q ($mg\,g^{-1}$)	b ($L\,mg^{-1}$)		q^0 ($mg\,g^{-1}$)	b ($L\,mg^{-1}$)	n		
pH_i 2.7											
WC	1.76	0.44	0.92	16.23	0.04	0.99	–	–	–	–	13.2
FLWC	0.80	0.49	0.94	10.73	0.03	0.98	–	–	–	–	7.9
FLWC1	0.75	0.46	0.95	8.15	0.03	0.99	–	–	–	–	6.5
FLPNC	1.26	0.47	0.95	14.69	0.03	0.99	–	–	–	–	11.5
GC	1.54	0.39	0.94	11.79	0.04	0.97	–	–	–	–	9.5
pH_i 6.8											
GC	35.0	0.28	0.65	115.8	0.36	0.77	109.6	0.52	0.021	0.99	112.3

adsorption on Oxisols and explained that the surface charge of the sorbent was changed by increased ionic strength [33]. Especially in case of pH close to pH_{zpc}, there was a characteristic pH below which increasing ionic strength increased Cd adsorption and above which the reverse occurred. This theory could also be applicable to explain the inflection behavior of Cd(II) adsorption on GC with increasing ionic strength.

3.3. Adsorption equilibrium

3.3.1. Isotherms

Figs. 7 and 8 show the adsorption isotherms of Cd(II) on various adsorbents at pH 2.7 and pH 6.8, respectively. Fig. 7 shows the isotherm of Cd(II) adsorption on GC at pH_i 2.7 and the fitted curves by Langmuir model. In comparison of the adsorption behaviors of different adsorbents at low C_e as shown in Fig. 7, GC was found to be the best with the highest adsorption amount q_e, reaching 1.65 at $C_e < 1.0\,mg\,L^{-1}$. The isotherms of other adsorbents appeared to be linear as the adsorption amount increased steadily with increasing C_e when the equilibrium concentration was less than $20\,mg\,L^{-1}$. Further increase in C_e resulted in increase in q_e at much slower rates which appeared to approach the saturation in adsorption. At the right end of the isotherms, the adsorption amount was clearly separated from each other and could be sequenced as: WC > FLPNC > GC > FLWC > FLWC1. Similar to Fig. 7, the isotherm of GC in Fig. 8 showed a sharp adsorption edge in the form of Langmuir type. Differently, the adsorption capacity was increased greatly when the initial pH was increased from 2.7 to 6.8.

3.3.2. Modeling

These isotherms were separately fitted by Freundlich, Langmuir and modified Langmuir isothermal models and the results are shown in Table 3.

Freundlich isothermal equation could be written as [2]:

$$q_e = K_F C_e^n \tag{4}$$

where q_e is the amount of the adsorbed substance on unit adsorbent ($mg\,g^{-1}$); C_e is the equilibrium concentration of adsorbate in solution ($mg\,L^{-1}$); K_F is the model constant indicating the monolayer adsorption capacity ($mg\,g^{-1}$); n is the model constant indicating the heterogeneity of the adsorption.

Langmuir isothermal equation is in the form of [2]:

$$q_e = \frac{QbC_e}{1 + bC_e} \tag{5}$$

where Q is the theoretical monolayer adsorption capacity of adsorbate on the adsorbent ($mg\,g^{-1}$); b is the model constant indicating the adsorption affinity.

Langmuir Equation can be modified in the form of Sips' model to account for the multilayered surface adsorption that is common on surfaces showing heterogeneous features [34,35]:

$$q_e = \frac{q^0(bC_e)^{1/n}}{1 + (bC_e)^{1/n}} \tag{6}$$

where q^0 is the adsorption capacity ($mg\,g^{-1}$); b indicates the adsorption equilibrium in terms of the ratio of adsorption rate over desorption rate; n is the model constant indicating the pattern of adsorption and is related to the degree of heterogeneity of a sorbent surface. Single layered adsorption is a particular case when $n = 1.0$.

Table 3 shows the predicted model constants. Langmuir model could better fit the test data for Cd(II) adsorption at pH_i 2.7 with much higher correlation coefficient (>0.97) than Freundlich model. The adsorption capacities of these adsorbents towards Cd(II) could be sequenced as: WC ($16.23\,mg\,g^{-1}$) > FLPNC ($14.69\,mg\,g^{-1}$) > GC ($11.79\,mg\,g^{-1}$) > FLWC ($10.73\,mg\,g^{-1}$) > FLWC1 ($8.15\,mg\,g^{-1}$), regarding the model constant Q. The experimentally

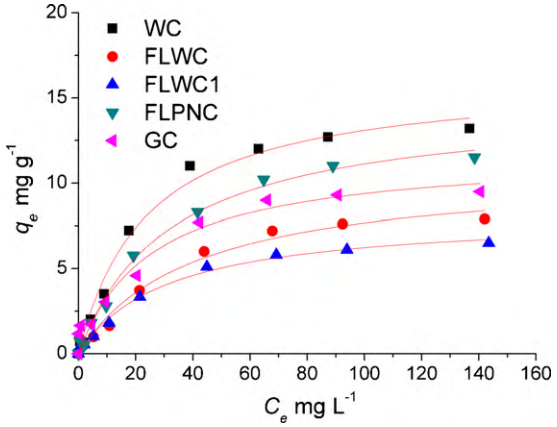

Fig. 7. Tested adsorption isotherms on various adsorbents and fitted curves by Langmuir model ($pH_i = 2.7$; dosage $1.0\,g\,L^{-1}$; $T = 25\,^{\circ}C$; $t = 24.0\,h$).

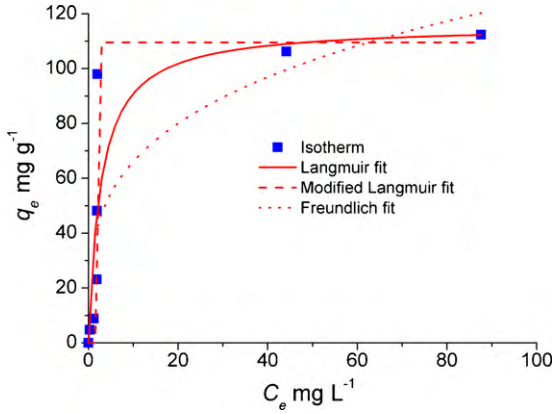

Fig. 8. Adsorption isotherm of GC and fitted curves ($pH_i = 6.8$; dosage $1.0\,g\,L^{-1}$; $T = 25\,^{\circ}C$; $t = 24.0\,h$).

determined sorption capacities are also listed in Table 3 for comparison. The calculated Langmuir sorption capacities were averagely higher than the determined data by 2–3 mg g^{-1}. The results seem satisfying since the theoretical capacity is always hard to reach in practice.

The Sips model was introduced to fit the test data of Cd(II) sorption on GC at pH 6.8. In view of the correlation coefficients, the Sips model could satisfactorily simulate the Langmuir shaped isotherm ($R^2 > 0.987$). The predicted adsorption capacity was close to the observed data, 109.6 mg g^{-1}. The predicted model constant n was 0.0209, indicating a high degree of surface heterogeneity in adsorption process. This speculation is in agreement with the observed morphology of GC as shown in the SEM photos in Fig. 1e–g.

3.4. Adsorption mechanism

3.4.1. Difference between adsorbents

Nitrogen is a critical element in all organisms, involved in all metabolic processes as well as in cellular structure and genetic coding. There are substantial changes in phenotype due to seasonal and ontogenetic development. N contents of different plant tissue can range from 0.03 to 7.0% of dry weight. Highest concentrations (3–7%) occur in young, actively growing tissues. During seasonal growth cycles, peak N concentrations occur whenever the cells of a plant tissue or organ are rapidly expanding in number and size [24]. The N content in wood is reported to be less than 0.2%, much less than that in leaves (1.5–5%) and grasses (0.9–4%) [24].

The pine needles used in this study were collected from the fallen leaves, and thus might have a reduced percent of N. Since the grass was mowed and was still in actively growing stage, the N content in GC might be higher than the pine needle char. This could explain the difference in amine groups and in Cd(II) adsorption capacities between these adsorbents.

Besides nitrogen, phosphorous also consists of the major functional groups of biomasses during the process of heredity. The phosphorus content of grass carp flesh was reported to be as high as 3.18% on a dry weight basis [25]. Our previous studies on pyrolyzed leaves confirmed the presence of phosphate in Pb(II) adsorption [19]. In this study, phosphate was specified in the IR spectra of GC at band 669 and 513 cm^{-1} as shown in Fig. 1, corresponding to the reported pyrolyzed leaf by the authors. But the strength of these patterns was very weak, indicating the low mass abundance in the adsorbent. As phosphate could react with many kinds of heavy metals to form insoluble precipitates, the presence of this group could greatly improve the adsorption performance of the adsorbent at low pHs. This might be correlated to the low Cd(II) uptake percent at pHs < 3.0.

3.4.2. Spectroscopy proofs

Fig. 9a shows the IR spectra of FLWC1 with and without Cd loading. No obvious change was found except for bands at 1383 and 423 cm^{-1} that appeared to be strengthened after Cd(II) adsorption. Similarly, these bands appeared in the IR of Cd(II) laden GC at pH$_i$ 2.7, as shown in lines b and d in Fig. 9b. Especially for the band at 1382 cm^{-1}, its intensity increased greatly with prolonged equilibration duration. This group was reported to be related to (1) ionogenic sulphonamide groups [36]; (2) bending vibration of methyl group [37]. In this paper we did not intend to exactly identify which speculation was correct, but tried to disclose a fact that the strong acidic solution indeed dissolved a portion of the GC adsorbent and thus resulted in the change of IR features of specific functional groups that were absent in the original form. This speculation further verified one conclusion of the kinetic studies which explained the abnormal reduction of adsorption amount with increasing equilibration duration.

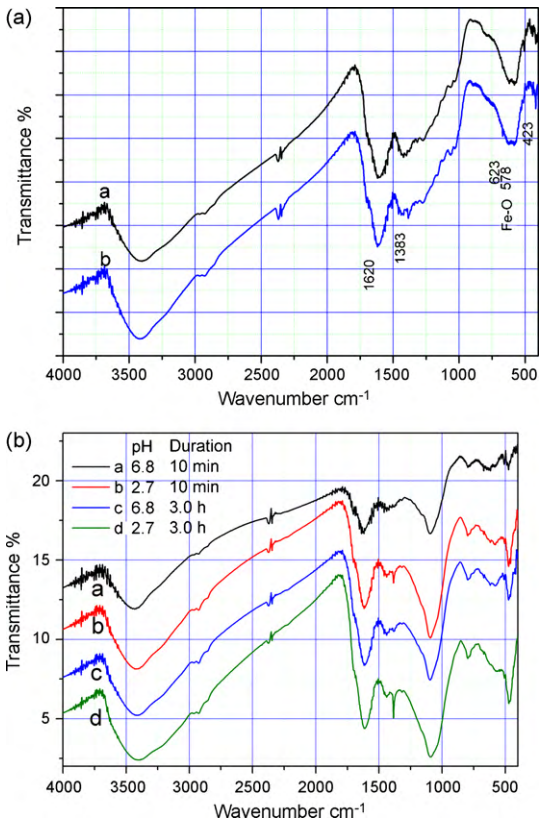

Fig. 9. (a) IR spectra of FLWC1 with and without Cd(II) loading (a: FLWC1; b: Cd(II) laden FLWC1 in terms of filter cake sampled from isothermal adsorption test at pH$_i$ 2.7). (b) IR spectra of filter cake of GC after kinetic test (a: pH$_i$ = 6.8, t = 10 min; b: pH$_i$ = 2.7, t = 10 min; c: pH$_i$ = 6.8, t = 3.0 h; d: pH$_i$ = 2.7, t = 3.0 h).

The bands relevant to carboxyl and/or amide group at 1710 and 1382 cm^{-1} were found decreased in absorption intensity after equilibrated with Cd(II) at neutral pHs. The broad band around 1660–1550 cm^{-1} could be assigned to NH group. These function groups are responsible for the strong buffering capacity of GC as shown in the pH effect test. The change in band intensity for NH group was obvious after GC contacted with Cd(II) solution (comparing line a to other three lines in Fig. 9b). Besides, it is also possible for Cd(II) to complex with the carboxyl and amide groups in the following forms:

$$\equiv COOH + Cd^{2+} + H_2O \Leftrightarrow \equiv COOCd(OH) + 2H^+ \quad (7)$$

$$\equiv NH_2 + Cd^{2+} + H_2O \Leftrightarrow \equiv NH_2Cd(OH)^+ + H^+ \quad (8)$$

Cd(II) was reported to be mainly coordinated with the carboxylic sites on surface of corncob since the adsorption capacity increased proportionally to the concentration of carboxylic sites [38]. The sorption capacities of Cd(II) on several soils could be decreased markedly in the presence of dissolvable organic matters [39]. The increase in the RCOOH concentration of juniper bark than wood (2.5 times more) was reported to give rise to Cd(II) adsorption on the former sorbent [9].

In acidic solutions, the iron oxide contained in GC might be dissolved and thus might decrease the relevant band intensity (at 578 cm^{-1}) in IR spectra, as confirmed by lines b and d in Fig. 9b. As a variable-charged mineral, iron oxide become active in Cd(II) adsorption only at pHs > pH$_{zpc}$ where the surface charge is negative [33]. At pH$_i$ 6.8, the following reaction might be present in the batch test:

$$\equiv FeOH + Cd^{2+} + H_2O \Leftrightarrow \equiv FeOCd(OH) + 2H^+ \quad (9)$$

Table 4
Maximum Cd(II) sorption capacities by various adsorbents from the literature.

Sorbent	Langmuir sorption capacity ($mg\,g^{-1}$)	pH	T (°C)	References
Acid soils of central Spain	0.86			[6]
Kaolin	1.46	6.8	25	[8]
Typical surface soils from Egypt and Greece	<2.00			[7]
Juniper wood	3.17			[9]
Natural corncob	5.12	6	25	[38]
Quaternary loess	9.37		25	[2]
Coastal sediments	10.01	5.5		[43]
Juniper bark	10.26			[9]
Carbon aerogel	15.53			[10]
Modified rice husk	31.15	6	25	
Sulphuric acid-treated wheat bran	43.10	5.4	25	[11,12]
Black gram (*Cicer arietinum*) husk	46.52			[45]
Oxidized corncob	55.20	6	25	[38]
Triethylenetetramine modified sugarcane bagasse	69.40			[41]
Nanometer AlO(OH) loaded on fiberglass	128.5			[42]
Grass char	11.79	2.7	25	This study
Grass char	115.8	6.8	25	This study

The broad band at $1620\,cm^{-1}$ relevant to amide group was weakened in intensity after immersed in solution at pH 2.7, indicating the following reactions:

$$\equiv NH_2 + H^+ \Leftrightarrow \equiv NH_3{}^+ \quad (10)$$

This mechanism could contribute to the buffering effect of GC to some extent.

The band appeared at $510\,cm^{-1}$ after Cd(II) adsorption could be assigned to disulphide group which was common in proteins and was considered responsible for the uptake of heavy metals by live cells [40].

3.5. Environmental significance

Table 4 shows the Cd(II) adsorption capacities of various reported adsorbents [41–43]. There are natural soils, clay minerals, natural organics and modified biomasses in this table. Natural soils showed the least Cd(II) adsorption capacities that were less than $10.0\,mg\,g^{-1}$. This could explain the high tendency of Cd(II) leaching from the polluted soil to the groundwater which could threaten the safety of the drinking water. Biomaterials generally demonstrate higher Cd(II) adsorption affinities than soils. Rice husk, plant barks, corncob and carbon aerogel were reported to be effective in Cd(II) adsorption. This provides an alternative treatment method to decrease the mobility of Cd(II) in the ground. GC was found to possess a higher Cd(II) adsorption capacity than most of the reported biomass based adsorbents. The nanomaterial AlO(OH) laden fiberglass had a larger adsorption capacity than our results, but the comparatively high cost in preparation limited its economic efficiency [42].

The yield efficiency of grass was determined at 31.25%. This value is a bit less than the reported value (36.25%) of *Firmiania simplex* L. [19]. Compared to similar adsorbents obtained from leaf, GC appears to be very stable without observable organic substances being extracted out after immersed in water. The aqueous solution remains clear while those previously prepared from leaves appeared to be brown.

The stability of GC could satisfy the requirement for the long-term application in landfill liner systems where an anaerobic condition dominates. Hilscher et al. reported a study on the microbial recalcitrance of char accumulated after calcinations of rye grass (*Lolium perenne*) at 350 °C under oxic conditions [44]. After aerobically incubated for 48 days at 30 °C, the grass-derived char showed a little extent of carbon mineralization (3.2%) from organic C to CO_2, indicating a very slow decomposition rate of the plant char under microbial attacks, comparable to those for soil organic matter (SOM). C-13 NMR spectroscopic analysis indicated structural changes during the microbial degradation in the form of decrease in O-alkyl/alkyl-C and increase in carboxyl/carbonyl C content by opening and oxidizing the aromatic ring structures [44]. Schulten et al. studied the fate of soil organic materials originated from grass root [20]. Corresponding to the conclusion of Hilscher et al., this study verified the stability of GC in the soil environment to resist microbial attacks [44]. Although its chemical constituents were a bit different from those of grass stem and leaves, the results might be helpful to evaluate the stability of the latter. The qualitative differences in the molecular composition of soil organic matter were clearly attributed to its rapid increase during the first 7 years of the experiment and largely originated from a relative enrichment of lignin dimmers [20]. That is to say, the decomposition of grass residue within a long period of 7 years resulted in some lignin dimmers. As shown by pyrolysis studies, most of these lignin dimmers (nearly 1/3) could be removed from the solid ash at temperatures less than 200 °C.

The grass char will be durable to resist natural decomposition when applied in engineering practice. The sensitive response to pH change in acidic conditions allows the easy removal of sorbed Cd(II) from the used sorbents. The sorbents are expected to be recycled after usage in wastewater treatment, for the further usage or for safe storage in landfill site. Otherwise, the leaching of enriched heavy metals on the sorbent would cause secondary pollution to the environment.

4. Conclusions

(1) Various biomaterials were pyrolyzed to prepare adsorbents for Cd(II) adsorption in this study. The grass char was found to be the best one with the highest sorption capacity at $115.8\,mg\,g^{-1}$ with solution pH at 6.8.
(2) The adsorption was very fast with the equilibrium achieved within 10 min for low concentration of Cd(II) at $2.5\,mg\,L^{-1}$ or within 120 min for high concentration at $10.0\,mg\,L^{-1}$. Dissolution of solvent in acid solution was found to gradually decrease the sorption capacity towards Cd(II) by releasing the sorbed Cd(II) from the sorbent.
(3) The adsorption was found to increase with increasing solute concentration, pH, contact time and sorbent dosage, but decrease with increasing ionic strength, especially for $CaCl_2$ solution. The most suitable condition for Cd(II) sorption on GC was determined as: $t > 120$ min, dosage $>10\,g\,L^{-1}$, $pH_i > 4.0$ and ionic strength <0.01 M.

(4) The spectroscopy and SEM studies revealed that the sorption of Cd(II) on GC was mainly involved with carboxyl and amine groups in terms of chemisorption.
(5) The charred biomaterials appear to be more stable than the original form and thus are promising in engineering practices.

Acknowledgement

This work was partly supported by Venture Business Laboratory of Utsunomiya University.

References

[1] K.T. Suzuki, C. Sasakura, M. Ohmichi, Binding of endogenous and exogenous cadmium to glutelin in rice grains as studied by HPLC/ICP-MS with use of a stable isotope, J. Trace Elem. Med. Biol. 11 (1997) 71–76.
[2] Y. Wang, X.W. Tang, Y.M. Chen, L.T. Zhan, Z.Z. Li, Q. Tang, Adsorption behavior and mechanism of Cd(II) on loess soil from China, J. Hazard. Mater. 172 (2009) 30–37.
[3] C. Xiong, C. Yao, L. Wang, J. Ke, Adsorption behavior of Cd(II) from aqueous solutions onto gel-type weak acid resin, Hydrometallurgy 98 (2009) 318–324.
[4] I. Riba, J. Blasco, N. Jimenez-Tenorio, T.A. DelValls, Heavy metal bioavailability and effects. I. Bioaccumulation caused by mining activities in the Gulf of Cadiz (SW, Spain), Chemosphere 58 (2005) 659–669.
[5] T.H. Christensen, Attenuation of Leachate Pollutants in Groundwater, 1st ed., E & FN SPON, London, 1992.
[6] S. Serrano, F. Garrido, C.G. Campbell, M.T. Garcia-Gonzalez, Competitive sorption of cadmium and lead in acid soils of Central Spain, Geoderma 124 (2005) 91–104.
[7] S.M. Shaheen, Sorption and lability of cadmium and lead in different soils from Egypt and Greece, Geoderma 153 (2009) 61–68.
[8] Y. Asci, M. Nurbas, Y.S. Acikel, Sorption of Cd(II) onto kaolin as a soil component and desorption of Cd(II) from kaolin using rhamnolipid biosurfactant, J. Hazard. Mater. 139 (2007) 50–56.
[9] E.W. Shin, K.G. Karthikeyan, M.A. Tshabalala, Adsorption mechanism of cadmium on juniper bark and wood, Bioresour. Technol. 98 (2007) 588–594.
[10] J. Goel, K. Kadirvelu, C. Rajagopal, V.K. Garg, Cadmium(II) uptake from aqueous solution by adsorption onto carbon aerogel using a response surface methodological approach, Ind. Eng. Chem. Res. 45 (2006) 6531–6537.
[11] A. Ozer, H.B. Pirincci, The adsorption of Cd(II) ions on sulphuric acid-treated wheat bran, J. Hazard. Mater. 137 (2006) 849–855.
[12] E.I. El-Shafey, Sorption of Cd(II) and Se(IV) from aqueous solution using modified rice husk, J. Hazard. Mater. 147 (2007) 546–555.
[13] Y. Daihyakka, *Zoysia japonica*, in: Y. Daihyakka (Ed.), The Exclusive Encyclopedia of Wild Plants, Hokuryūkan, Heisei, Tokyo, 1992, p. 357.
[14] H.C. Butterman, M.J. Castaldi, Influence of CO_2 injection on biomass gasification, Ind. Eng. Chem. Res. 46 (2007) 8875–8886.
[15] D.K. Shen, S. Gu, The mechanism for thermal decomposition of cellulose and its main products, Bioresour. Technol. 100 (2009) 6496–6504.
[16] O. Senneca, Kinetics of pyrolysis, combustion and gasification of three biomass fuels, Fuel Process. Technol. 88 (2007) 87–97.
[17] H. Kawamoto, M. Murayama, S. Saka, Pyrolysis behavior of levoglucosan as an intermediate in cellulose pyrolysis: polymerization into polysaccharide as a key reaction to carbonized product formation, J. Wood Sci. 49 (2003) 469–473.
[18] X.W. Tang, Z.Z. Li, Y.M. Chen, Adsorption behavior of Zn(II) on calcinated Chinese loess, J. Hazard. Mater. 161 (2009) 824–834.
[19] Z. Li, X. Tang, Y. Chen, L. Wei, Y. Wang, Activation of *Firmiana simplex* leaf and the enhanced Pb(II) adsorption performance: equilibrium and kinetic studies, J. Hazard. Mater. 169 (2009) 386–394.
[20] H.R. Schulten, P. Leinweber, G. Reuter, Initial formation of soil organic-matter from grass residues in a long-term experiment, Biol. Fertil. Soils 14 (1992) 237–245.
[21] Z. Li, S. Imaizumi, T. Katsumi, X. Tang, Pyrolysing wood into carbons for Cr(VI) adsorption: performances compared to mineral adsorbents, in: J. Zhang, Y. Yao (Eds.), 4th Sino-Japan Symposium on Geotechnical Engineering, Okinawa, Japan, 2010.
[22] R.M. Rowell, Handbook of Wood Chemistry and Wood Composites, Taylor & Francis, CRC Press Boca Raton, FL, United States, 2005.
[23] G.N. Richards, G. Zheng, Pyrolysis gasification of chars from wood containing iron and copper sulfates, Energy Fuels 9 (1995) 136–140.
[24] W.J. Mattson, Herbivory in relation to plant nitrogen content, Annu. Rev. Ecol. Syst. 11 (1980) 119–161.
[25] J.G. Stanley, Nitrogen and phosphorus balance of grass carp, Ctenopharyngodon idella, Fed Elodea, Egeria densa, Trans. Am. Fish. Soc. 103 (1974) 587–592.
[26] P. Gerardin, M. Petric, M. Petrissans, J. Lambert, J.J. Ehrhrardt, Evolution of wood surface free energy after heat treatment, Polym. Degrad. Stabil. 92 (2007) 653–657.
[27] Y.S. Ho, G. McKay, A comparison of chemisorption kinetic models applied to pollutant removal on various sorbents, Trans. Inst. Chem. Eng. 76 (1998) 332–340.
[28] F.C. Wu, R.L. Tseng, R.S. Juang, Initial behavior of intraparticle diffusion model used in the description of adsorption kinetics, Chem. Eng. J. 153 (2009) 1–8.
[29] G. McKay, M.S. Otterburn, A.G. Sweeney, The removal of colour from effluent using various adsorbents. III. Silica: rate processes, Water Res. 14 (1980) 15–20.
[30] Z.Z. Li, X.W. Tang, Y.M. Chen, Y. Wang, Sorption behavior and mechanism of Pb(II) on Chinese loess, J. Environ. Eng. ASCE 135 (2009) 58–67.
[31] Y.N. Yang, Y. Chun, G.Y. Sheng, pH-Dependence of pesticide adsorption by wheat-residue-derived black carbon, Langmuir 20 (2004) 6736–6741.
[32] J.J. Wang, D.L. Harrell, Effect of ammonium, potassium, and sodium cations and phosphate, nitrate, and chloride anions on zinc sorption and lability in selected acid and calcareous soils, Soil Sci. Soc. Am. J. 69 (2005) 1036–1046.
[33] R. Naidu, N.S. Bolan, R.S. Kookana, K.G. Tiller, Ionic-strength and ph effects on the sorption of cadmium and the surface-charge of soils, Eur. J. Soil Sci. 45 (1994) 419–429.
[34] S. Al-Asheh, F. Banat, R. Al-Omari, Z. Duvnjak, Predictions of binary sorption isotherms for the sorption of heavy metals by pine bark using single isotherm data, Chemosphere 41 (2000) 659–665.
[35] S.C. Tsai, K.W. Juang, Y.L. Jan, Sorption of cesium on rocks using heterogeneity-based isotherm models, J. Radioanal. Nucl. Chem. 266 (2005) 101–105.
[36] S.N. Gladkikh, R.R. Shifrina, Y.M. Popkov, S.F. Timashev, V.P. Bazov, S.V. Timofeyev, Modification of perfluorinated sulpho-cationite membranes with amines, Polym. Sci. U.S.S.R. 26 (1984) 456–462.
[37] E.A. Romanenko, B.V. Tkachuk, Infrared spectra and structure of thin polydimethylsiloxane films, J. Appl. Spectrosc. 18 (1973) 188–192.
[38] R. Leyva-Ramos, L.A. Bernal-Jacome, I. Acosta-Rodriguez, Adsorption of cadmium(II) from aqueous solution on natural and oxidized corncob, Sep. Purif. Technol. 45 (2005) 41–49.
[39] Z.G. Li, C.Z. Bian, X.L. Jie, Characteristic of Cd sorption in the copper tailings wasteland soil by amended dissolved organic matter from fresh manure and manure compost, Afr. J. Biotechnol. 6 (2007) 227–234.
[40] H. Sugeta, A. Go, T. Miyazawa, Vibrational-spectra and molecular-conformations of dialkyl disulfides, Bull. Chem. Soc. Jpn. 46 (1973) 3407–3411.
[41] L.V.A. Gurgel, L.F. Gil, Adsorption of Cu(II), Cd(II) and Pb(II) from aqueous single metal solutions by succinylated twice-mercerized sugarcane bagasse functionalized with triethylenetetramine, Water Res. 43 (2009) 4479–4488.
[42] G.H. Liu, P.P. Wang, Q. Liu, W. Han, Removal of Cd(II) by nanometer AlO(OH) loaded on fiberglass with activated carbon fiber felt as carrier, Chin. J. Chem. Eng. 16 (2008) 805–811.
[43] S. Oh, M.Y. Kwak, W.S. Shin, Competitive sorption of lead and cadmium onto sediments, Chem. Eng. J. 152 (2009) 376–388.
[44] A. Hilscher, K. Heister, C. Siewert, H. Knicker, Mineralisation and structural changes during the initial phase of microbial degradation of pyrogenic plant residues in soil, Org. Geochem. 40 (2009) 332–342.
[45] A. Saeed, M. Iqbal, R.G.J. Edyvean, S.I. Zafar, Scaled-up biosorption of Cd in single, binary (Cd + Pb, Cd + Ni), and ternary (Cd + Pb + Ni) solutions by black gram (Cicer arietinum) Husk in a stirred tank bioreactor, Fresenius Environ. Bull. 16 (2007) 1600–1607.